10.1

DOPPLER LIDAR OBSERVATIONS OF THE COHERENT STRUCTURES IN THE INTERNAL BOUNDARY LAYER

Ryoko Oda[1], Hironori Iwai[1], Yasuhiro Murayama[1], Shoken Ishii[1], Kohei Mizutani[1], Toshikazu Itabe[1], Nobumitsu Tsunematsu[2], Izumi Yamada[3], Naoki Matayoshi[4], Dai Matsushima[5], Weiming Sha[6], Takeshi Yamazaki[6] and Toshiki Iwasaki[6]
1. National Institute of Information and Communications Technology, Tokyo, Japan
2. Chiba University, Chiba, Japan
3. Electronic Navigation Research Institute, Tokyo, Japan
4. Japan Aerospace Exploration Agency, Tokyo, Japan
5. Chiba Institute of Technology, Narashino, Japan
6. Tohoku University, Sendai, Japan

1. INTRODUCTION

It is important to investigate the characteristics of turbulent organized structure (TOS) developed in near surface layer since it is considered to control the vertical exchange processes of momentum, heat and other scalars between the ground surface and atmosphere (e.g., Wilczak and Tillman, 1980). Many studies have investigated the nature of TOS using numerical simulation, wind-tunnel experiment and outdoor experiment. Adrian et al. (2000) expected from their wind tunnel experiment that the predominant structures within the inertial and outer layer over flat walls are represented by very large low-speed streaks with packets of hairpin vortices. Inagaki and Kanda (2010) also observed a streaky structure of low momentum region in the outdoor reduced urban scale model experiment (COSMO). Although these streaky structures with orderly different sizes seem to be qualitatively similar, such similarity has not been vilified quantitatively yet.

We conducted Coherent Doppler lidar (CDL) observations over Sendai Airport on June 2007 using two lidars; one is developed by Electronic Navigation Research Institute (ENRI) and another is by National Institute of Information and Communications Technology (NICT). Doppler lidar enables us to observe the wind field on a slice of several kilometers radius. Therefore, it can detect larger scale structures than in the conventional experimental approaches (e.g, Newsom et al. 2008; Iwai et al. 2008).

In this study, we detected the turbulent structures developed above the real urban boundary layer and examine their predominant length scale by comparing with the observation in the outdoor scale model experiment (Inagaki 2008) which has smaller fetch and roughness length.

* *Corresponding author address*: Ryoko Oda, National Institute of Information and Communivations Technology, 4-2-1 Nukui-Kitamachi, Koganei-shi, Tokyo, 184-8795 JAPAN;
e-mail: oda.r@nict.go.jp

2. OBSERVATIONS

2.1 *Site Description*

This experiment was conducted in Sendai Airport which is located in Natori, Miyagi, facing the Pacific Ocean (38.14°N, 140.92°E). Therefore, the regional flow field is usually affected by sea breeze.

ENRI lidar (Komatsubara and Kaku 2005) and NICT lidar (Ishii et al. 2007) were stationed on the rooftop of ENRI's Iwanuma branch building (16.7m above the ground) at 2.5 km west and 4 km west from the Pacific coast, respectively (Fig. 1).

2.2 *Data Processing*

The atmospheric observation was conducted at Sendai airport from 9 to 20 June 2007. ENRI lidar operates at an eye-safe wavelength of 1.54 μm, with 0.2 mJ pulse energy, at a pulse repetition frequency (PRF) of 4 kHz. It has a range resolution of 29.9 m, and minimum and maximum ranges are 80 m and up to 2.5 km, respectively. NICT lidar operates at an eye-safe wavelength of 2.012 μm, with 7 mJ pulse energy, at a PRF of 100 Hz. It has a range resolution

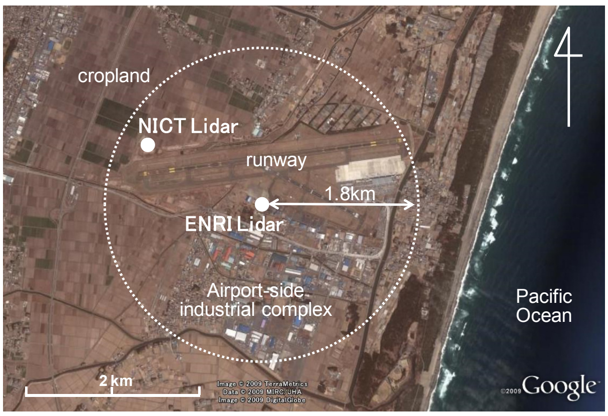

Fig.1 Observation site. Measurement range of ENRI Lidar is circled in the figure.

Table 1 Specification of ENRI Lidar and NICT Lidar

	ENRI	NICT
Transceiver unit	Mitsubishi Electric Corp.	Coherent Technologies Inc.
Scanner control & data processing system	Mitsubishi Electric Corp.	NICT
wave length	1.54 μm	2.012 μm
pulse energy	0.2 mJ/pulse	7 mJ/pulse
pulse repetition frequency	4 kHz	100 Hz
accumulated shot number	500	50
range resolution	29.9 m	90 m
minimun range	80.0 m	315 m
miaximum range	2.472 km	~ 10 km
scan rate	6.0 deg/sec	0.4 deg/sec

of 90 m, and minimum and maximum ranges are 315 m and up to 10 km, respectively. The radial velocity and signal-to-noise ratio (SNR) in each range were determined as the averages over 500 laser pulses for ENRI lidar and 50 laser pulse for NICT lidar. Table 1 shows the list of the specification of above two lidars.

ENRI lidar performed full 360 degree Constant-Altitude Plan Position Indicator (CAPPI) scans at elevation angles from 0.5 to 5.0 degree in 0.5 degree increments in the day time. In order to focus on the structure of TOS near the surface, the PPI scan data at elevation angle of 1.0 degree (from 22.0 to 48.6 m above the ground) were used on June during 13:01 to 14:26 JST (every 12 min scan). NICT lidar performed the 135 degree azimuth Range Height Indicator (RHI) scan (i.e., parallel to the sea breeze flow) at almost same time as the ENRI lidar observation (19 June 12:39-12:47 JST).

In this experiment, the atmospheric stability was slightly unstable (Iwai et al. 2008), which was estimated from the vertical profiles of the wind velocity and air temperature measured by the heliborne sensors of Japan Aerospace Exploration Agency (JAXA) (Okuno et al. 2002; Matayoshi et al. 2005).

3. RESULTS

3.1 *Horizontal distribution of radial velocity fluctuation*

Figure 2 (a) shows the radial velocity observed by PPI scan at 13:01, in which positive velocities indicate the flow away from the lidar, and negative velocity indicates the flow come close to the lidar. At this time, the winds blow from the southeast (136 degree azimuth) at 5.7 m s^{-1}. This flow field is driven by the sea breeze from the Pacific Ocean.

To extract the turbulent structures from the datasets of PPI scans, radial velocity fluctuations are calculated by subtracting the mean radial velocity, which is estimated from the Velocity Azimuth Display (VAD) method, from the radial velocity (Fig. 2 (b)). The horizontal distribution of the radial velocity fluctuations shows the existence of the streaky

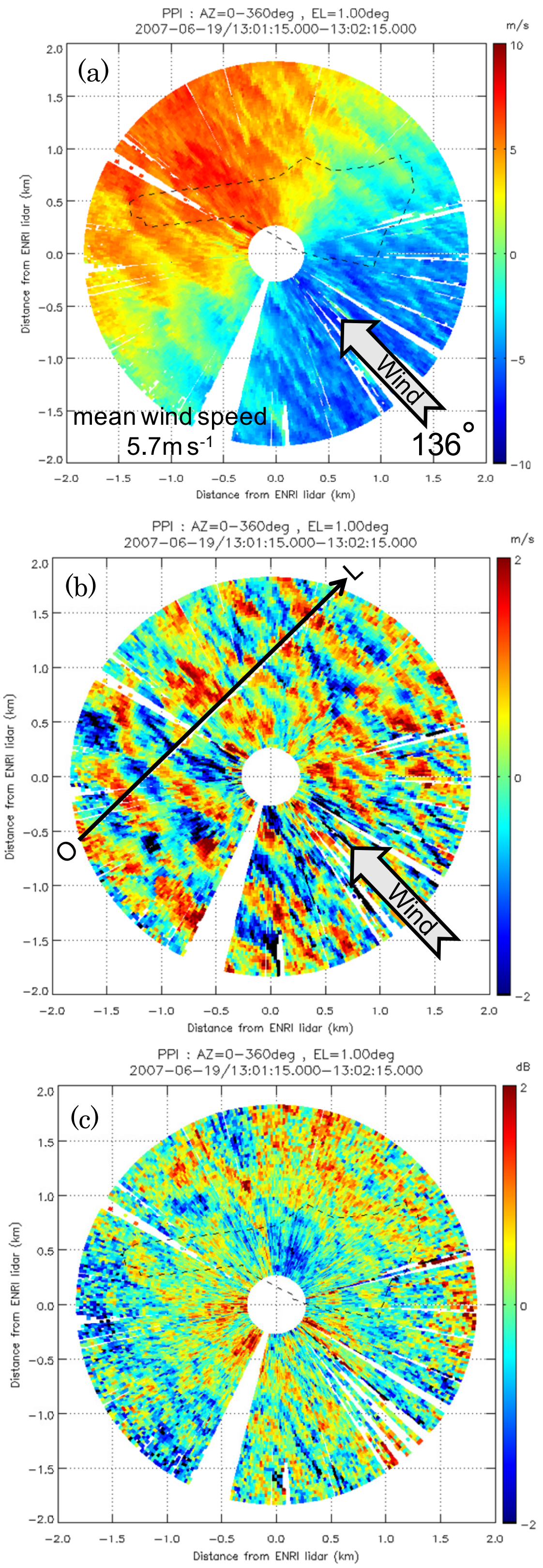

Fig.2 Horizontal distribution of (a) radial velocity, (b) radial velocity fluctuation and (c) rSNR observed by PPI scan at 13:01 JST.

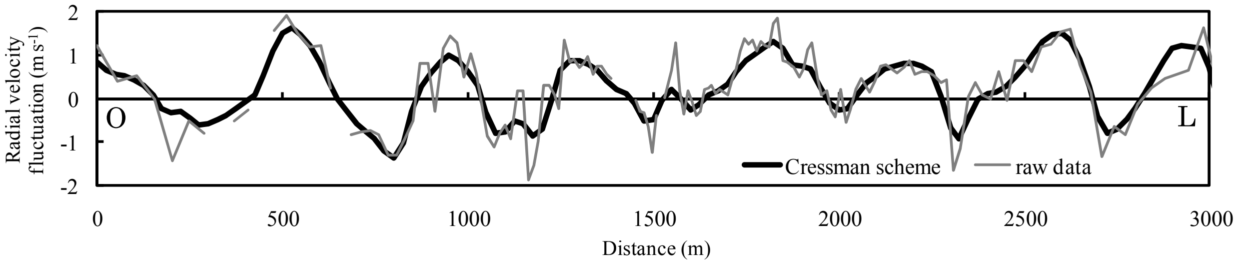

Fig.3 The spanwise distribution of radial velocity fluctuation at 800 m leeward from ENRI lidar (O-L line in Fig. 2 (b)). Gray and bold lines indicate the raw values and the interpolated values using Cressman scheme, respectively.

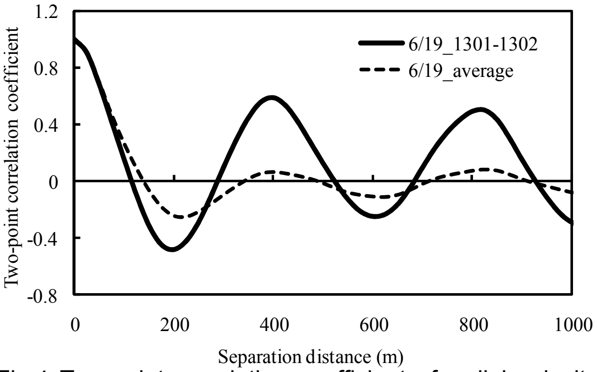

Fig.4 Two-point correlation coefficient of radial velocity plotted in the separation distance along the spanwise direction at 13:01 JST (bold line), and that from the ensemble average of all PPI scans data from 13:01 to 14:26 JST.

structures elongated along the streamwise direction.

Similarity, figure 2 (c) shows the fluctuations of the range collected SNR (hereafter rSNR), which are calculated from the following two steps; (1) subtracting mean rSNR averaged in a same radius, (2) subtracting mean rSNR averaged in a range direction, from the observed rSNR. The resulted rSNR distribution also shows the streaky structure as well as the radial velocity fluctuations.

3.2 *The intervals of the streaks*

In this study, we focused on the intervals of the streak structures as one of the quantitative characteristics of the turbulent structure.

Figure 3 shows the spanwise distribution of the fluctuation velocity at 800 m leeward from ENRI lidar (O-L line in Fig. 2 (b)). Since the data points of the measurement is not aligned along straight line of the spanwise direction, this data was interpolated using a Cressman scheme (Cressman 1959). In this figure, the gray line is the distribution of radial velocity fluctuation using the nearest values from the spanwise straight line, and the bold line is the one interpolated on the line. The setting of a Cressman grid in this analysis was 50 m horizontal grid spacing and 40 m height of the horizontal plane. Based on this interpolated datasets, the intervals of the streaks were estimated by a two-point correlation analysis:

$$R(dx) = \frac{\overline{u'(x)u'(x+dx)}}{\sqrt{\overline{u'^2(x)}}\sqrt{\overline{u'^2(x+dx)}}}, \qquad (1)$$

where x is a location; dx is the distance between the two measurement points; u' is the radial velocity fluctuations; $\overline{}$ means the ensemble average.

The solid line in Fig. 4 indicates the two-point correlation coefficient of the interpolated radial velocity fluctuation plotted on the separation distance along the spanwise direction. There are correlation peaks at specific separation distances which would indicate the intervals of the streaks seen in Fig. 3. The intervals of the streaks were estimated about 400 m. The second peek seen at about 800 m would be the harmonic component of the primal peak. The calculated two-point correlation coefficients were ensemble averaged among all PPI scans data obtained from 13:01 to 14:26 JST. This also resulted that the primal peak is appeared at 400 m separation distance.

The same analysis was conducted also for the datasets of rSNR, however, we cannot see a clear peaks as seen in the case of radial velocity fluctuation.

3.3 *Relationships between the intervals of the streaks and the boundary layer heights*

Some studies have examined the relationships between the intervals of the streaks and the atmospheric boundary layer height (z_i) (e.g., Lin et al. 1997). However, it is not completely confirmed in atmospheric field observations since it is difficult to carry out the simultaneous observation of horizontal distribution and vertical profile of the wind field in the range of several km. We observed the vertical profile of radial wind velocity using NICT lidar as described in 2.2. Figure 5 shows the distribution of rSNR on a vertical cross-section at 12:39-12:47 JST. The internal boundary layer height (δ) can be detected at about 220 m over Sendai Airport because there is sharp gradient of the rSNR profile (Melfi et al. 1985). Moreover, the depth of the atmospheric boundary layer was about 700 m where the wind direction changed (Iwai et al. 2008).

The horizontal scale of the turbulent structure within the mixed layer is expected to be $1.5z_i$ based on the mixed-layer scaling (Kaimal et al. 1976). If we

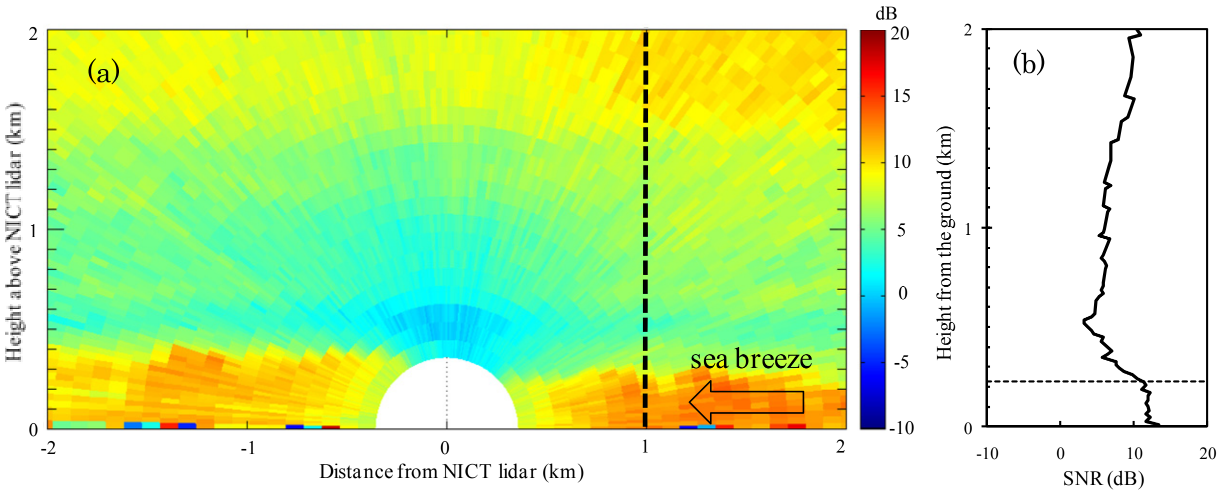

Fig.5 (a) The vertical cross-section of rSNR at 12:39-12:47 JST. (b) The vertical profile of rSNR at 1 km windward from NICT lidar (dashed line at Fig. 5 (a)).

assume that the interval of the streaks follows the mixed-layer scaling, it is estimated to be about 1000 m in this observation period. This is different from the value estimated from the two point correlation.

To explore the correct scaling parameter for the interval of the streaks, we compared the value in a different experiment, which is obtained in the outdoor reduced urban scale model experiment (Inagaki and Kanda 2010).

Inagaki and Kanda (2010) indicated that the interval of the streak structures is usually about 20 m under near-neutrally stratification in daytime, when z_i and δ are usually about 1000 m and less than 10 m, respectively. If the intervals of the streaks are normalized by z_i and δ, they reduce to an order of 10^{-2} and 10^{0}, respectively.

The same scale analysis is also applied to the values of the current lidar observation. The interval of the streaks becomes an order of 10^{-1} using z_i, and an order of 10^{0} using δ. The intervals of streaks are one-order different if they are scaled by z_i, and it become a same order if they are scaled by δ. Therefore, the intervals of the streaks seem to not relevant for the atmospheric boundary layer height but for the internal boundary layer height.

3.4 *Variation of the intervals of the streaks along the streamwise direction*

Figure 6 shows the two-point correlation coefficient plotted for the separation distance along the spanwise direction. The difference of the lines distinguishes the location of the measurement along the fetch at 400-1000 m leeward apart from ENRI lidar. Although the correlation peeks of any streamwise locations appear at 375-450 m, we cannot see a clear dependency on the length of the fetch in this figure. Therefore, about 400 m interval of the streaks is expected to be a representative value over this area. This is possibly because the internal boundary layer

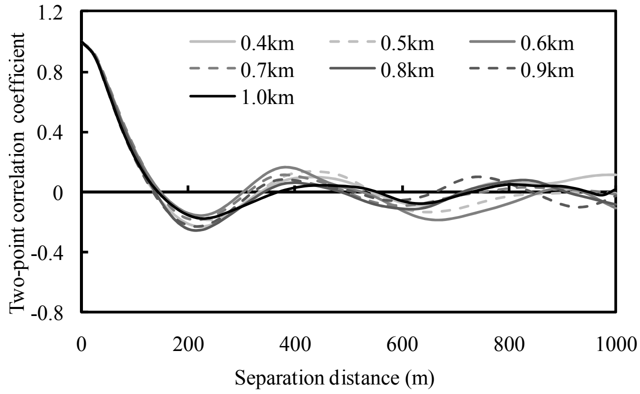

Fig.6 Two-point correlation coefficient of the interpolated spanwise component of the streaks from the ensemble average of all PPI scans data from 13:01 to 14:26 JST at leeward distance from ENRI lidar.

has already sufficiently developed until the flow arrives at this area, and the horizontal heterogeneity of the surface conditions in the experimental area is not so large to disturb the streaky structures.

4. CONCLUSIONS

The Coherent Doppler lidar observations were conducted using two lidars, which are the Electronic Navigation Research Institute (ENRI)'s lidar and the National Institute of Information and Communications Technology (NICT)'s lidar, to investigate the turbulent organized structure developed over Sendai Airport. The horizontal distribution of the radial velocity fluctuations revealed the occurrence of the streak structures which are elongated along the main stream. The intervals of the streaks in the spanwise direction were estimated about 400 m from the two-point correlation analysis. The present analysis resulted that the relevant scale of the interval of the streaks is not the atmospheric boundary layer height but the internal boundary layer height.

ACKNOWLEDGEMENTS

This research was financially supported by the Japan Ministry of Education, Culture, Sports, Science and Technology (PI: T. Iwasaki, 19204046). The authors thank Dr. Inagaki (Tokyo Institute of Technology, Japan) for his useful comments and suggestions.

REFERENCES

Adrian, R. J., Meinhart, C. D. and Tomkins, C. D., 2000: Vortex organization in the outer region of the turbulent boundary layer, *J. Fluid Mech.*, **422**, 1-54, doi:10.1017/S0022112000001580.

Cressman, G. P., 1959: An operational objective analysis system, *Mon. Weather Rev.*, **87**, 367-374.

Ingakaki, A., 2008: Atmospheric turbulence over an array of massive cubes, PhD Thesis, Tokyo Institute of Technology.

Inagaki, A. and Kanda, M., 2010: Organized structure of active turbulence developed over an array of cubes within the logarithmic layer of atmospheric flow, *Bounday-Layer Meteorol.*, **135**, 209-228, doi:10.1007/s10546-010-9477-0.

Ishii, S., Sasaki, K., Mizutani, K., Aoki, T., Kanno, H., Matsushima, D., Sha, W., Noda, A., Sawada, M., Ujiie, M., Matsuura, Y. and Iwasaki, T., 2007: Temporal evolution and spatial structure of the local easterly wind “Kiyokawa-dashi” in Japan PART I: coherent Doppler lidar observations, *J. Meteor. Soc. Jpn.*, **85**, 797-813, soi:10.2151/jmsj.85.797.

Iwai, H., Ishi, S., Tsunematsu, N., Mizutani, K., Murayama, Y., Itabe, T., Yamada, I., Matayoshi, N., Matsushima, D., Sha, W., Yamazaki, T. and Iwasaki, T., 2008: Dual-Doppler lidar observation of horizontal convective rolls and near-surface streaks, *Geophys. Res. Lett.*, **35**, L14808, doi:10.1029/2008GRL034571.

Kaimal, J. C., Wyngaard, J. C., Haugen, D. A., Coté, O. R. and Izumi, Y., 1976: Turbulence structure in the convective boundaly layer, *J. Atmos. Sci.*, **33**, 2152-2169.

Komatsubara, T. and Kaku, N., 2005: The status of wake vortex research in Japan, *Proceedings of the 13th Coherent Laser Radar Conference*, Kamakura, Japan, 140-143, 16-21 October.

Lin, C.-L., Moeng, C.-H., Sullivan, P. P. and McWilliams, J. C., 1997: The effect of surface roughness on flow structures in a neutrally srarified planetary boundary layer flow, *Phys. Fluids*, **9**, 3235-3249.

Matayoshi, N., Inokuchi, H., Yazawa, K. and Okuno, Y., 2005: Development of an airborne ultrasonic velocimeter and its application to helicopters, *Proceedings of the AIAA Atmospheric Flight Mechanics Conference and Exhibit*, San Francisco, California, AIAA 2005-6118, 15-18 August.

Melfi, S.H., Spinhirne, J. D., Chou, S.-H. and Palm, S. P., 1985: Lidar observations of vertically organized convection on the planetary boundary layer over the ocean, *J. Clim. Appl. Meteor.*, **24**, 806-821.

Newsom, R., Calhoun, R., Ligon, D. and Allwine, J., 2008: Linearly organized turbulence structures observed over a suburban area by dual-Doppler lidar, *Bounday-Layer Meteorol.*, **127**, 111-130, doi:10.1007/s10546-007-9243-0.

Okuno, Y., Matayoshi, N., Terui, Y., Wakairo, K., Hozumi, K., Inokuchi, H. and Funabiki, K., 2002: Development of a research helicopter MuPAL-ε, *Tech. Memo. TM-764, Natl. Aerospace Lab., Tokyo* (In Japanese).

Wilczak, J. M. and Tillman, J. E., 1980: The three-dimensional structure of convection in the atmospheric surface layer, *J. Atmos. Sci.*, **37**, 2424-2443.